

Verteporfin- and sodium porfimer-mediated photodynamic therapy enhances pancreatic cancer cell death without activating stromal cells in the microenvironment

Jingjing Lu
Bhaskar Roy
Marlys Anderson
Cadman L. Leggett
Michael J. Levy
Brian Pogue
Tayyaba Hasan
Kenneth K. Wang

Verteporfin- and sodium porfimer-mediated photodynamic therapy enhances pancreatic cancer cell death without activating stromal cells in the microenvironment

Jingjing Lu,^{a,b,†} Bhaskar Roy,^{a,†} Marlys Anderson,^a Cadman L. Leggett,^a Michael J. Levy,^a Brian Pogue,^c Tayyaba Hasan,^d and Kenneth K. Wang^{a,*}

^aMayo Clinic and Foundation, Barrett's Esophagus Unit, Division of Gastroenterology and Hepatology, Rochester, Minnesota, United States

^bPeking University Third Hospital, Gastroenterology Department, Beijing, China

^cDartmouth College, Thayer School of Engineering, Hanover, New Hampshire, United States

^dHarvard School of Medicine, Massachusetts General Hospital, Boston, Massachusetts, United States

Abstract. The goal of our study was to determine the susceptibility of different pancreatic cell lines to clinically applicable photodynamic therapy (PDT). The efficacy of PDT of two different commercially available photosensitizers, verteporfin and sodium porfimer, was compared using a panel of four different pancreatic cancer cell lines, PANC-1, BxPC-3, CAPAN-2, and MIA PaCa-2, and an immortalized non-neoplastic pancreatic ductal epithelium cell line, HPNE. The minimum effective concentrations and dose-dependent curves of verteporfin and sodium porfimer on PANC-1 were determined. Since pancreatic cancer is known to have significant stromal components, the effect of PDT on stromal cells was also assessed. To mimic tumor–stroma interaction, a co-culture of primary human fibroblasts or human pancreatic stellate cell (HPSCs) line with PANC-1 was used to test verteporfin-PDT-mediated cell death of PANC-1. Two cytokines (TNF- α and IL-1 β) were used for stimulation of primary fibroblasts (derived from human esophageal biopsies) or HPSCs. The increased expression of smooth muscle actin (α -SMA) confirmed the activation of fibroblasts or HPSC upon treatment with TNF- α and IL-1 β . Cell death assays showed that both sodium porfimer- and verteporfin-mediated PDT-induced cell death in a dose-dependent manner. However, verteporfin-PDT treatment had a greater efficiency with 60x lower concentration than sodium porfimer-PDT in the PANC-1 incubated with stimulated fibroblasts or HPSC. Moreover, activation of stromal cells did not affect the treatment of the pancreatic cancer cell lines, suggesting that the effects of PDT are independent of the inflammatory microenvironment found in this two-dimensional culture model of cancers. © The Authors. Published by SPIE under a Creative Commons Attribution 4.0 Unported License. Distribution or reproduction of this work in whole or in part requires full attribution of the original publication, including its DOI. [DOI: [10.1117/1.JBO.24.11.118001](https://doi.org/10.1117/1.JBO.24.11.118001)]

Keywords: pancreatic cancer; photosensitizer; verteporfin; sodium porfimer; photodynamic therapy; fibroblast.

Paper 190074R received Mar. 18, 2019; accepted for publication Oct. 18, 2019; published online Nov. 18, 2019.

1 Introduction

Pancreatic cancer is the fourth leading cause of cancer-related deaths in the United States, with an estimated 43,090 deaths in 2017.¹ Pancreatic ductal adenocarcinoma (PDAC) is the most common form of pancreatic cancer and is notoriously difficult to treat. Currently, surgical resection is the only potentially curative treatment available for early stage PDAC patients, and chemotherapy and radiation therapy have limited success in lengthening patients' survival with later stage disease.² However, more than half (52%) of patients are diagnosed at advanced stages and are not eligible for surgical resection, resulting in a 5-year survival rate of only 3%.¹ New diagnostic and therapeutic modalities are urgently needed to improve the survival of PDAC patients beyond the minimal benefit that they receive today.

Photodynamic therapy (PDT)³ is a light-based therapeutic modality, which has been approved in the US, Japan, China, Korea, UK, and several other European countries for the

treatment of head and neck, bladder, esophageal, and endobronchial cancers.^{4,5} Upon activation with a specific wavelength of light and depending on the interval between drug administration and photoradiation, PDT-induced cell death can be mediated by cellular and vascular modes. An activated photosensitizer generates highly reactive molecular species and singlet oxygen, which induce tumor cell death by direct cytotoxicity and indirect effects, such as microvascular damage, apoptosis, autophagy, and immune responses.^{5,6} Apoptotic [intrinsic (mitochondria-mediated) and extrinsic (the death receptor-mediated)]^{6,7} and necrotic pathways⁸ play a role in PDT-mediated cell death. Perhaps most importantly, PDT has been reported by various groups as an adjuvant to chemotherapy to enhance cell death *in vitro* and *in vivo*^{3,9–11} with broad-based killing efficiency. A report by Huang et al.¹² suggested that PDT in combination with chemotherapy overcomes selection pressures of therapy-resistant clones usually noted in chemotherapeutic modalities and killed cancer and cancer stem-like cells agnostically. Clinically, intraluminal PDT has been used to treat superficial lesions since the effective depth of light penetration is limited to <10 mm; whereas intratumor light delivery (interstitial PDT) is used in bulky tumors having a tumor depth >10 mm.¹³ With the

*Address all correspondence to Kenneth K. Wang, E-mail: wang.kenneth@mayo.edu

[†]These authors are cofirst authors.

development of laser treatment fibers, PDT has been demonstrated to control lesions of localized pancreatic tumors, and its safety and efficacy in preclinical and clinical studies have been reported.^{6,7,14–16}

In this study, we focused on comparing the effect of two photosensitizers—the first being sodium porfimer (commonly known as Photofrin), one of the first commercially available photosensitizers used in head and neck, esophageal, and endobronchial cancer in the past. Previous preclinical studies have demonstrated that pancreatic cancer cells are sensitive to sodium porfimer-PDT, and clinical studies have suggested it as a potential treatment for pancreatic cancer,¹⁵ cholangiocarcinoma,⁷ and intraductal papillary mucinous neoplasm.¹⁷ However, sodium porfimer is clinically difficult to use since it has a long cutaneous photosensitization duration of at least 4 to 6 weeks.^{5,6} The impact on quality of life limits its usefulness in the treatment of pancreatic cancer patients.

Verteporfin, the other photosensitizer used in this study, is a second-generation photosensitizer, with a liposomal formulation of benzoporphyrin derivative monoacid ring-A. This drug has already been approved for clinical use for age-related macular degeneration⁵ and has substantially reduced light sensitivity due to rapid clearance rates. Data generated from a phase I/II clinical study in advanced pancreatic cancer patients have shown that verteporfin-PDT induced tumor necrosis locally and is feasible and safe for clinical implementation.⁸ The goal in this study was to compare the effect of verteporfin-mediated PDT with sodium porfimer-mediated PDT on multiple PDAC cell lines as well as on benign ductal epithelium. Insight was sought into the effectiveness of both photosensitizers in the treatment of pancreatic cancer cells *in vitro*. Therefore, four commonly studied human pancreatic epithelial/ductal adenocarcinoma cell lines, PANC-1, CAPAN-2, BxPC-3, and MIA PaCa-2, derived from primary tumors¹⁸ and the benign pancreatic ductal epithelial line, HPNE, were selected for this study. The selected epithelial/ductal adenocarcinoma cell lines represent the varying grades, histological differentiations, and immune-cytochemical features associated with pancreatic cancer,^{19,20} whereas HPNE was created from normal human pancreatic ducts and was immortalized by transduction with a retroviral expression vector containing the hTERT gene. PANC-1, CAPAN-2, and MIA PaCa, but not BxPC-3, are characterized by frequent mutations in KRAS (v-kinase2 Kirsten rat sercoma viral oncogene homolog), TP53, and CDKN2A (P16 INK4a), contributing to the growth, tumorigenic properties, and chemoresistance.^{20–24} BxPC-3 and CAPAN-2 cells are both derived from mucin (MUC)-producing cancers. The aberrant expression of various isoforms of MUC plays a role in the development and progression of pancreatic cancer.^{25,26} Finally, various associated cells and extracellular components surround the pancreatic tumors, forming a complex network of pro- and antitumor components and confer a protective effect against chemotherapy and cytotoxicity.²⁷ Activated fibroblasts and stellate cells expressing α -smooth muscle actin (α -SMA) are the predominant cells in stroma and produce extracellular matrix (ECM) products and cytokines, as well as growth factors associated with desmoplastic reaction. They are the origin of cancer-associated fibroblasts, promoting tumor proliferation, progression, invasion, metastasis, and chemoresistance.^{27–29} A few studies have examined the influence of the stroma on the therapeutic effect of PDT.³⁰ Celli³¹ demonstrated that PDT was able to destroy fibroblasts in a three-dimensional (3-D) co-culture model. In this study, we

developed an *in-vitro* co-culture model comprised of pancreatic cancer cells with activated fibroblasts or human pancreatic stellate cells (HPSCs) in cell inserts to illustrate their influence on PDT to address whether there was a tissue-specific difference between fibroblasts derived from low-grade esophageal dysplasia and HPSCs from pancreatic origin.

2 Materials and Methods

2.1 Cell Culture

Four human pancreatic cell lines, PANC-1, MIA PaCa-2, CAPAN-2, and BxPC-3, and one human immortalized pancreatic ductal epithelium cell line, HPNE (ATCC, Manassas, Virginia), were cultured in appropriate media and according to the recommended guidelines of ATCC.

Dulbecco's modified Eagle medium (DMEM) with high glucose for PANC-1 and MIA PaCa-2 cell lines, DMEM with low glucose for the HPNE cell line, and RPMI for the BxPC-3 cell line, as well as sodium pyruvate, sodium bicarbonate, penicillin-streptomycin, glucose, and puromycin were obtained from Sigma (St. Louis, Missouri). PANC-1, MIA PaCa-2, CAPAN-2, and BxPC-3 were maintained in media supplemented with 10% heat-activated fetal bovine serum (FBS) (HyClone, Logan, Utah), 0.1% antibiotic solution (v/v), 2.5% horse serum (ATCC, Manassas, Virginia) for MIA PaCa-2 and 1 mM sodium pyruvate for MIA PaCa-2 and BxPC-3. CAPAN-2 cells were maintained in modified McCoy 5A media base (ATCC) supplemented with 10% FBS and 0.1% antibiotic solution (v/v). The normal (also known as control) pancreatic cells, HPNE, were maintained in media supplemented with M3 Base F (INCELL, San Antonio, Texas), 5.5 mM glucose (750 ng/ml), and 10 ng/ml epidermal growth factor (Millipore, Burlington, Massachusetts).

Cells were grown at 37°C in a humidified incubator with $\pm 5\%$ CO₂. Fibroblasts were isolated and grown from primary human Barrett's esophagus (BE) biopsy samples. Those cells were isolated from BE patients with varying degrees of dysplasia undergoing endoscopy. Briefly, the esophageal biopsies were minced into ~ 2 mm³ fragments and the primary culture was grown in "Barrets-Plus" media, a modified keratinocyte media as previously described.³² HPSC were cultured by the method as previously described.³³ Fibroblasts or HPSCs were stimulated by the addition of 50 ng/ml human TNF- α protein and 10 ng/ml human recombinant IL-1 β protein (both from R&D systems, Minneapolis, Minnesota) to the media, while the other unstimulated group continued with media alone for 96 h. After sufficient numbers of fibroblasts or HPSCs were grown, they were split into two groups and replated into new dishes. One group of fibroblasts was stimulated by the addition of human TNF- α (50 ng/ml) and human recombinant IL-1 β (10 ng/ml) to the media, while the unstimulated group continued with media alone for 96 h.

2.2 Co-Culture Assay

PANC-1 cells were plated on coverslips in three 12-well plates for 24 h with $\sim 25,000$ cells per well, prior to inserts being added. The stimulated, nonstimulated fibroblasts and HPSC were rinsed and plated into two 6 inserts with $\sim 15,000$ cells per insert (Falcon Cell Culture Inserts, Corning, Inc., New York) for each cell line. Each set of 6 inserts was placed in two plates of PANC-1 [Fig. 1(b)], while the third plate of PANC-1 contained no inserts or fibroblasts and was set as a control. All cells were

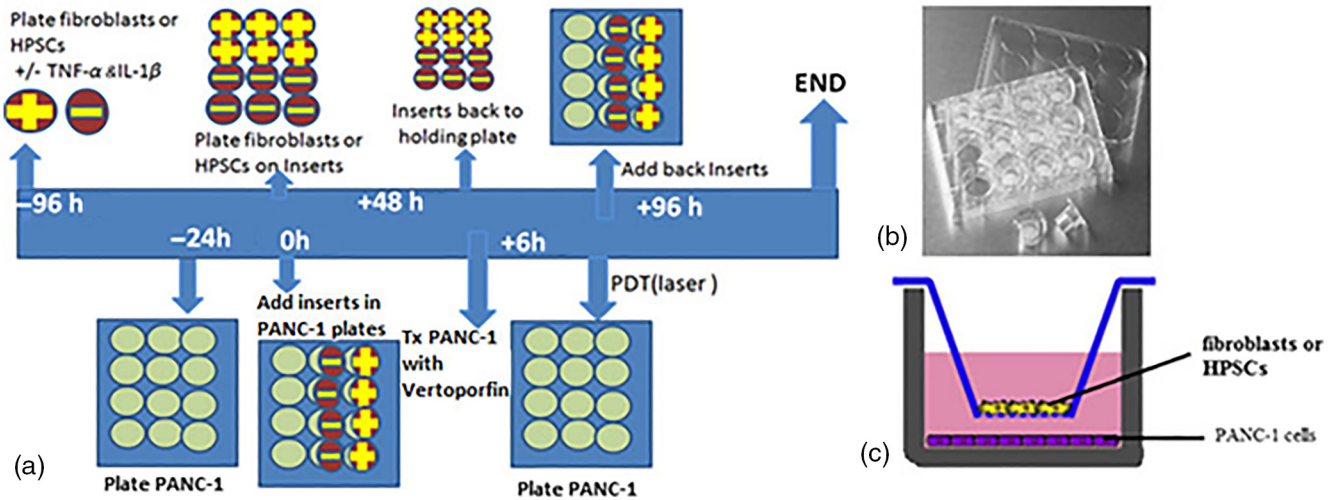


Fig. 1 (a) The flowchart showing fibroblasts or HPSCs inserts over PANC-1 plates for verteporfin-PDT. (b) Picture of 12-well culture insert. (c) Schematic diagram of co-culture of the fibroblasts or HPSCs insert over PANC-1 cells.

incubated for another 48 h. The inserts were taken out prior to incubating PANC-1 cells with verteporfin.

2.3 Photosensitizing Agent

Verteporfin (Tocris Bioscience, Bristol, United Kingdom) was dissolved in DMSO at a 0.5 mg/ml concentration, whereas sodium porfimer (Frontier Scientific, Logan, Utah) was dissolved in sterile 0.1% NaOH at a 5 mg/ml concentration. Both photosensitizers were reconstituted according to the manufacturers' instruction and stored in brown tubes in the dark in a 4°C refrigerator until use. Immediately prior to PDT experiments, a range of each photosensitizing agent at different concentrations was prepared in test media. The test media consisted of 10% FBS DMEM cell culture media diluted with phosphate-buffered saline (PBS) in a ratio of 1:10.

2.4 Preliminary Experiments for Optimal Photodynamic Therapy Dose

A series of preliminary experiments with verteporfin- and sodium porfimer-mediated PDT in PANC-1 cells were conducted to determine the optimal PDT settings. The light source used for the experiments was equipped with a medium pressure xenon lamp of 300 W (Oriol Corp., Stratford, Connecticut, now Newport Corporation) holding dichroic and bandpass filters to modulate the range of the spectral output. An internally housed cooling fan regulated the temperature at the set point (as room temperature), thus decreasing the thermal effect. According to our previous study,³ the peak wavelength of 665 nm was set with an irradiance of 0.50 W/cm² as measured by volume absorbing calorimetry, for verteporfin treatment to achieve a light dose of 60 J/cm². A bandpass filter with a peak at 630 nm was used for sodium porfimer to achieve equal irradiance and light dose of 60 J/cm² for both photosensitizers. Light irradiation was calculated using the Thorlabs Photodiode power sensor with a 9.5-mm aperture compensated for the responsivity of the sensor over the necessary wavelengths. Sensor linearity is determined to be 0.5%. The minimum concentrations of sodium porfimer and verteporfin that could effectively induce complete cell death in PANC-1 cells were determined. The toxicity study

was conducted using concentrations of sodium porfimer of 0, 0.10, 0.25, 0.50, 1.00, 2.50, 5.00, and 10.00 μ g/ml and verteporfin of 0, 0.001, 0.0025, 0.005, 0.025, 0.05, and 0.1 μ g/ml.

2.5 Cell Lines Cultured with the Photosensitizer

First, each pancreatic cell line (PANC-1, MIA PaCa-2, CAPAN-2, BxPC-3, and HPNE) was trypsinized and replated into two 8-well chamber slides (slides A and B) with \sim 25,000 cells per well. After incubation for 48 h, the cells in slide A were incubated with test media containing incremental concentrations of 0, 0.10, 0.25, 0.50, 1.00, 2.50, 5.00, and 10.00 μ g/ml sodium porfimer, whereas cells in slide B were incubated with test media containing incremental concentrations of 0, 0.001, 0.0025, 0.005, 0.025, 0.05, and 0.1 μ g/ml verteporfin. Cells were incubated with these photosensitizers for 6 h. All cells were washed with PBS twice to remove the excess photosensitizer and were replaced by the same amount of test media without photosensitizer followed by photoradiation. Each slide was illuminated for 2 min with the peak wavelength of 665 and 630 nm and a light dose of 60 J/cm² as previously described.³ After PDT, test media were removed and the cells were rinsed once with PBS. All wells were filled with the respective growth medium described above and incubated for 96 h [Fig. 1(a)].

2.6 Cytotoxicity Assays

SYTOX green and Hoechst 33342 (both from Invitrogen) were added to the media in each well after a 96-h incubation period as described earlier.³ SYTOX green is a nuclear chromosome fluorescent stain that penetrates dead cells through their compromised cellular membranes. In this solution, dead cells were labeled with green fluorescence and the rest of the cells were marked with blue fluorescence staining from Hoechst. Using a fluorescent Axiovert microscope (Zeiss, Germany), the percentage of dead cells was determined as a measure of cytotoxicity. We counted the number of fluorescent SYTOX green staining cells in a set of 100 Hoechst staining cells. A minimum

of 300 cells were recorded for each well to determine overall cytotoxicity.

2.7 Dark- and Light-Dependent Toxicity

To determine the dark toxicity, PANC-1 cells were incubated with a range of concentrations of the both photosensitizers, then washing twice with PBS and incubated with photosensitizer-free fresh medium for 18 and 96 h. For assaying the light-dependent cytotoxicity, PANC-1 cells in the absence of any photosensitizer were illuminated as described above and then incubated for 24 h. Calcein AM-ethidium homodimer-based live/dead assay was performed to determine the cytotoxicity, and live/dead cells were enumerated using Celigo (Nexelom Inc., Lawrence, Massachusetts). In the range of concentrations assayed for dark toxicity of the two photosensitizers, the three highest concentrations, including lethal dose (LD) (100% cell death) were tested (Fig. S2 in the [Supplementary Material](#)). In addition, the temperature of growth media with corresponding photosensitizers was monitored before and after illumination to record temperature increment to determine light-dependent cytotoxicity in the experimental model.

2.8 Immunofluorescence

Before the fibroblasts or HPSCs were put into the inserts, we prepared two chamber slides (one line for stimulated and one line for unstimulated) and two centrifuge slides for each cell type. One slide was incubated overnight, to allow reattachment of the cells, followed by PBS rinsing and air drying. A representative sample of the cells went into the inserts, while the second slide was grown parallel with the experimental plates. At the end of the experiment, the membranes from stimulated and unstimulated inserts with fibroblasts and HPSCs, the parallel grown fibroblasts and HPSCs chamber slides, and the air-dried preinsert slide were stained for α -SMA. HPSCs were also stained for glial fibrillary acidic protein (GFAP). Briefly, they were fixed in 100% methanol for 10 min at -20°C and permeabilized with 1% Tween 20 in 0.1% bovine serum albumin (BSA)/PBS for 10 min. All slides were blocked with 10% goat serum in 0.1% BSA/PBS, for 1 h. They were incubated with mouse anti- α -SMA or anti-GFAP (Abcam, Cambridge, Massachusetts), followed by goat anti-mouse IgG (α -SMA) or goat anti-rabbit IgG (GFAP) for 1 h each with the appropriate staining controls. All slides and membranes used coverslip with ProLong gold containing 4',6-diamidino-2-phenylindole (DAPI). Stained cells were imaged with an AxioVert microscope (Carl Zeiss), equipped with a digital camera and Axio Vision software. Myofibroblasts were characterized by immunofluorescence positivity for α -SMA. We visually verified that stimulated fibroblasts showed more positive staining for α -SMA than unstimulated fibroblasts.

2.9 Statistical Analysis

Parametric data were expressed as means and standard deviations. Paired Student's *t*-test and one-way ANOVA (post-hoc test between groups) were used to analyze parametric data. The Wilcoxon rank sum test and Kruskal-Wallis test followed by the Dunn-Bonferroni test for post-hoc comparisons were used to analyze the nonparametric data. All of the statistical analyses were performed using SPSS 19.0 software package. The level of statistical significance was set at $P < 0.05$.

3 Results

The cytotoxic effect of photosensitizers in the complete absence of illumination is referred to as dark toxicity. Overall, no significant dark cytotoxicity was observed (Fig. S2 in the [Supplementary Material](#)) in either of the photosensitizers. For verteporfin-PDT, the average cell death (in percentage of total live + dead) obtained was 7.79% in the untreated control, which remained relatively unchanged in increased concentrations of the compound after 18 h of incubation. A similar trend was observed after 96 h of incubations as well as with a slight increase in overall dead cell percentage (8.39% for untreated control). In the sodium porfimer treated group, a small change in cell death was observed ($*P = 0.01$) (7.6% for untreated control versus 6.36% for 10.0 $\mu\text{g}/\text{ml}$), at the highest concentration only, which was also the LD (100% cell death) for sodium porfimer. After 96 h, the cell death was consistent with results obtained from verteporfin treatment and no significant change on cell death was observed (Fig. S2 in the [Supplementary Material](#)). Light-dependent toxicity employed by our experimental setup showed that a 2 min (5.06% for 665 nm and 4.56% for 630 nm) or even longer 4 min (5.37% for 665 nm and 5.55% for 630 nm) exposure did not have any significant effect of cell death (5.4% in absence of light). Also there was no increment in temperature of the culture media of the *in-vitro* experimental model after 2 min (experimental design) or even a longer period of time (4 min) (data not shown) suggesting minimum or no effect of light-induced cytotoxicity.

The LD (100% lethal dose) of sodium porfimer and verteporfin in PANC-1 was determined, and ranges of different concentrations of these two compounds were tested. At a concentration of 10.0 $\mu\text{g}/\text{ml}$ (8.48 nmol/ml) or higher of sodium porfimer and a concentration of 0.10 $\mu\text{g}/\text{ml}$ (0.14 nmol/ml) or higher of verteporfin, nearly 100% cell death was achieved. It was apparent that verteporfin is much more efficient in inducing cell death. Both photosensitizers demonstrated dose-dependent cytotoxicity. Next, we compared the efficacy and efficiency of sodium porfimer and verteporfin between all pancreatic cell lines and a benign pancreatic epithelial cell line. Furthermore, we investigated if stimulated fibroblasts or HPSCs inserts had any effect on treatment of PANC-1 cells with verteporfin-PDT.

At the highest concentration of 10.0 $\mu\text{g}/\text{ml}$ (8.48 nmol/ml), nearly 100% cell death was achieved by sodium porfimer in all five pancreatic cell lines. The LD50 (50% lethal dose) of sodium porfimer showed that HPNE cells were the most sensitive to sodium porfimer PDT (Table 1), followed by PANC-1, BxPC-3, MIA PaCa-2, and CAPAN-2 cells. When comparing the sodium porfimer dosages, HPNE cells were more sensitive to sodium porfimer PDT than pancreatic cancer cell lines, whereas there was no significant difference in sensitivity between the pancreatic cancer cell lines [Fig. 2(a)]. CAPAN-2 cells were less sensitive than HPNE cells at concentrations of 0.25, 0.50, and 1.00 $\mu\text{g}/\text{ml}$ of sodium porfimer ($P = 0.025$, 0.013, and 0.002, respectively). MIA PaCa-2 cells were less sensitive than HPNE at concentrations of 0.50 and 1.00 $\mu\text{g}/\text{ml}$ of sodium porfimer ($P = 0.013$ and 0.002, respectively). BxPC-3 was less effective than HPNE at concentrations of 1.00 and 2.50 $\mu\text{g}/\text{ml}$ of sodium porfimer ($P = 0.011$ and 0.046, respectively). PANC-1 is less sensitive than HPNE at a concentration of 0.50 $\mu\text{g}/\text{ml}$ of sodium porfimer ($P = 0.027$) [Fig. 2(b)].

At a concentration of 0.10 $\mu\text{g}/\text{ml}$ (0.14 nmol/ml) verteporfin-PDT caused almost complete cell death in all five pancreatic

Table 1 LD50 of pancreatic cell lines of sodium porfimer and verteporfin-PDT. After 6 h of incubation with sodium porfimer or verteporfin followed by photoradiation at a light dose of 60 J/cm² (PDT) for 2 min and incubation for another 96 h, comparable dead cell rates were found in pancreatic cell lines. LD50 was counted by SPSS19.0 software.

Cell lines	Photosensitizer			
	Sodium porfimer (μg/ml)		Verteporfin (μg/ml)	
	LD50	95% CI	LD50	95% CI
HPNE	0.44	0.32 to 0.58	0.005	0.005 to 0.006
BxPC-3	0.85	0.59 to 1.21	0.008	0.006 to 0.012
CAPAN-2	1.29	0.90 to 1.87	0.016	0.013 to 0.019
MIA PaCa-2	1.02	0.60 to 1.75	0.015	0.011 to 0.020
PANC-1	0.77	0.50 to 1.16	0.007	0.006 to 0.008

cell lines. The LD50 showed the similar results as sodium porfimer PDT (Table 1). The HPNE cells were most sensitive followed by PANC-1, BxPC-3, MIA PaCa-2, and CAPAN-2 cells.

In contrast to sodium porfimer PDT, the pancreatic cancer cell lines showed different sensitivities to the verteporfin-PDT [Fig. 2(a)]. HPNE and PANC-1 are the most sensitive to verteporfin-PDT, followed by BxPC-3, MIA PaCa-2, and CAPAN-2 [Fig. 2(c)]. BxPC-3 is less sensitive than HPNE cells at concentrations of 0, 0.001, and 0.01 μg/ml of verteporfin ($P = 0.009$, 0.043, and 0.010 respectively), but it is significantly more sensitive than CAPAN-2 cells at concentrations of 0, 0.001, 0.0025, and 0.050 μg/ml of verteporfin ($P = 0.001$, 0.002, 0.032, and 0.011, respectively). The CAPAN-2 cells were less sensitive than HPNE cells at concentrations of 0.0025, 0.005, 0.010, 0.025, 0.050, and 0.100 μg/ml of verteporfin ($P = 0.020$, 0.034, 0.002, 0.004, 0.001, and 0.031 respectively) and less sensitive than PANC-1 cells at concentrations of 0.005, 0.100, 0.0250, 0.050, and 0.100 μg/ml of verteporfin ($P = 0.011$, 0.016, 0.003, 0.000, and 0.003, respectively). MIA PaCa-2 cells were less sensitive than HPNE cells at concentrations of 0.0050, 0.0100, 0.0250, 0.0500, and 0.1000 μg/ml of verteporfin ($P = 0.016$, 0.000, 0.005, 0.025, and 0.03, respectively) and PANC-1 cells at concentrations of 0.0050, 0.0100, 0.0250, 0.0500, and 0.1000 μg/ml of verteporfin ($P = 0.003$, 0.001, 0.004, 0.008, and 0.003, respectively) [Fig. 2(d)].

Both verteporfin and sodium porfimer induced cell death in a dose-dependent manner, and they had similar efficacy. However, the verteporfin apparently had higher efficacy than sodium porfimer because of significantly lower concentrations of sodium

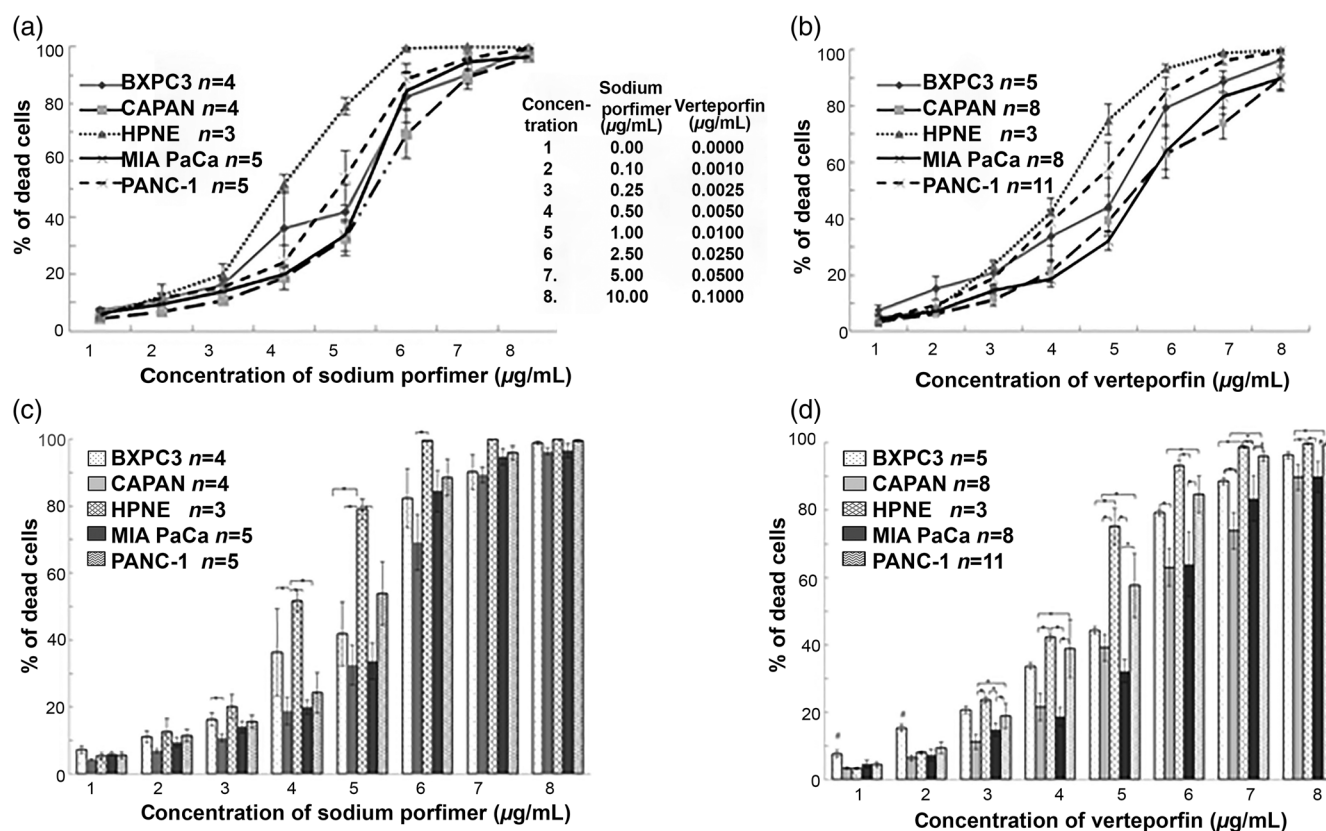


Fig. 2 Sodium porfimer- or verteporfin-mediated PDT-induced cell death in five pancreatic cell lines. Using 6-h incubation with photosensitizer followed by photoradiation at light dose of 60 J/cm² (PDT) in 2 min, assay was performed 96 h post-PDT. (a) Line graphs show that HPNE cells were more sensitive to sodium porfimer PDT than pancreatic cancer cell lines. (b) Comparable death rates in pancreatic cancer cells versus HPNE cells with sodium porfimer PDT ($*P < 0.05$). (c) Bar graphs show the sensitivity to verteporfin-PDT for HPNE, PANC-1, BxPC-3, and CAPAN-2/MIA. (d) Relative cell death rates for each pancreatic cell line. (Dead cell rate of BxPC-3 was statistically higher than other cell lines in control and at a concentration of 0.0010 μg/ml of verteporfin; $*P < 0.05$).

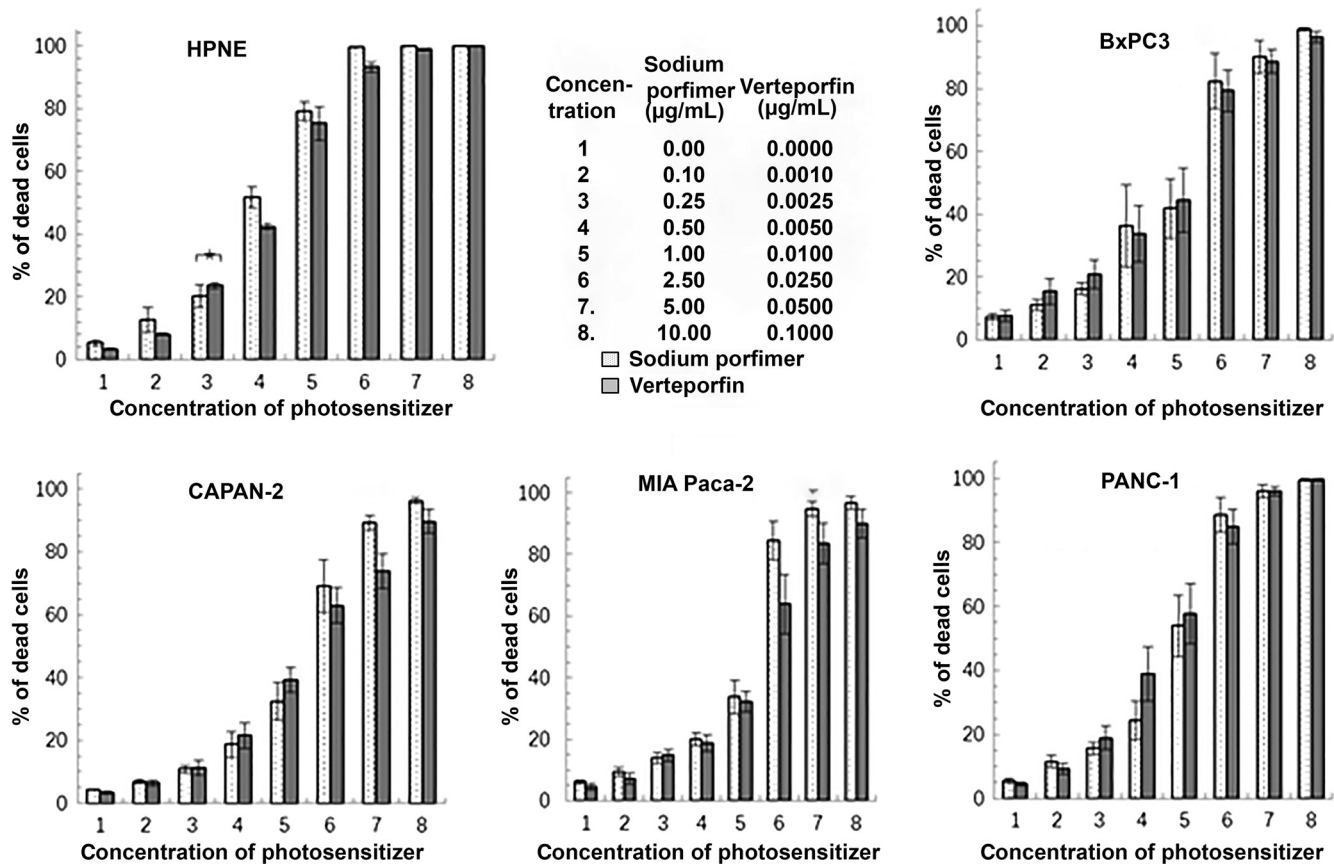


Fig. 3 Verteporfin- versus sodium porfimer-mediated PDT-induced cell death in five pancreatic cell lines. The death rate of HPNE cells with treatment at a concentration of 0.0025 $\mu\text{g}/\text{ml}$ of verteporfin was slightly lower than that of 0.25 $\mu\text{g}/\text{ml}$ sodium porfimer treatment ($P < 0.05$). No statistically significant differences existed between other cell lines.

porfimer (0.14 nmol/ml versus 8.48 nmol/ml); verteporfin-PDT showed almost similar cytotoxicity as sodium porfimer in all cell lines (Table 1). The only exception was HPNE, which was more sensitive to a concentration of 0.0025 $\mu\text{g}/\text{ml}$ of verteporfin than to a concentration of 0.25 $\mu\text{g}/\text{ml}$ of sodium porfimer ($t = 2.86$, $P = 0.046$, Fig. 3).

GFAP is a marker of quiescent HPSCs³⁴ and α -SMA is a marker of activated fibroblasts or HPSC. Immunofluorescence results showed that the expression of GFAP was positive for all HPSCs but that it was lower in HPSCs stimulated by IL-1 β and TNF- α than in unstimulated HPSCs [see Fig. 4(a)], which correlated with the decreased expression of GFAP in myofibroblast-like phenotype transformation. By contrast, the expression of α -SMA was higher in fibroblasts or HPSCs stimulated with IL-1 β and TNF- α than in unstimulated fibroblasts or HPSCs [see Fig. 4(a)]. These results indicate that the fibroblasts and HPSCs change to a myofibroblast-like phenotype after stimulation.

The cytotoxic effect, based on the percentage of dead PANC-1 cells at each concentration of verteporfin-PDT, demonstrated a positive dose-response correlation [Figs. 4(b) and 4(c)]. The percentage of dead PANC-1 cells was slightly different at each concentration of verteporfin. The PANC-1 cell death in the presence of stimulated fibroblasts or HPSCs was lower than the cell death in the presence of unstimulated fibroblasts or the control group, which may suggest a trend toward a protective effect of stimulated fibroblasts on cancer cell death in verteporfin-PDT treatment (but not statistically significant).

4 Discussion

Depending on their photophysical, chemical, biological properties (i.e., cellular uptake, distribution, and tumor selectivity), and quantum efficiency, every photosensitizer has certain benefit to be used in PDT; therefore, selecting the most appropriate photosensitizers for the best clinical outcome requires a careful analysis of all the factors. In this study, a similar illumination setting was used to compare and contrast the two photosensitizers (verteporfin and sodium porfimer), with their PDT-related properties that showed a range of resistance and sensitivity on various pancreatic cancer cell lines *in vitro*. Sodium porfimer is the most commonly used photosensitizer in the United States for gastrointestinal applications. Previous studies have demonstrated that sodium porfimer preferentially accumulated in the mitochondria of cancer cells to induce direct damage to the cells, thereby reducing cell viability and proliferation. Even though sodium porfimer has a useful absorption peak at 630 nm, a maximum absorption peak at this wavelength cannot be reached. Moreover, being a complex mixture of molecules with poor tissue selectivity, a higher concentration of the drug is needed to induce cell death.^{5,35} A higher concentration of the drug causes a longer retention time in the patient's system rendering them photosensitive.^{36,37} Verteporfin-PDT has been approved for clinical use in patients with age-related macular degeneration for two decades. It has rapid pharmacokinetics and high singlet oxygen yield with low skin photosensitivity.⁴ Preclinical and clinical studies showed that verteporfin-PDT is a potent therapy

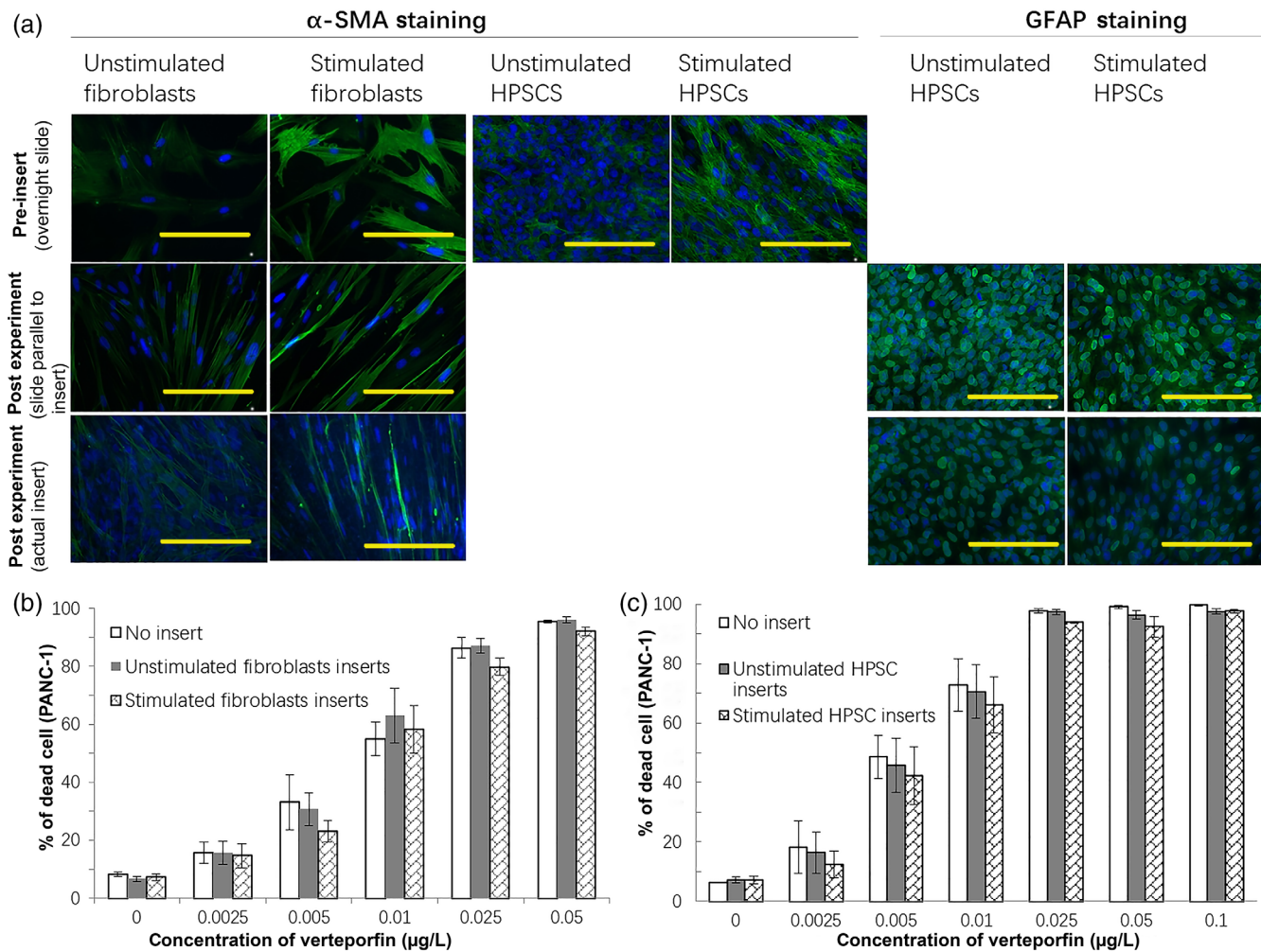


Fig. 4 (a) Representative immunofluorescence results showed that the expression of α -SMA was higher in fibroblasts or HPSCs stimulated by IL-1 β and TNF- α than in unstimulated cells, both pre-PDT and post-PDT. GFAP expression was positive in HPSCs, and the expression of GFAP was lower in stimulated HPSCs and postexperiment HPSCs. Nuclei stained blue with DAPI. α -SMA and GFAP labeled in green by alex488. (Scale bar: 200 μ). (b) The percentage of death cell plotted with serial concentrations of verteporfin with or without fibroblasts inserts. (c) The percentage of death cell plotted with serial concentrations of verteporfin with or without HPSCs inserts.

for pancreatic cancer.^{9,10,38,39} We demonstrated that verteporfin is a highly efficient cytotoxic modality compared with sodium porfimer, as it induces almost 100% cell death with a much lower concentration (0.1 μ g/ml (0.14 nmol/ml) photoradiation dose of 60 J/cm². Verteporfin has been reported to induce cancer cell death *in vitro* and *in vivo* through various mechanisms, as previously described.^{10,39,40} First, verteporfin can induce mitochondria-mediated apoptosis; second, it suppresses the proliferation of PANC-1 cells by arresting G1 phase and induces apoptosis by downregulating cyclinD1 and cyclinE1, modulation of Bcl-2 family proteins; and third, it inhibits angiogenesis and vasculogenic mimicry via suppression of Ang2, MMP2, VE-cadherin, and α -SMA expression. In addition, verteporfin impairs Yes-associated protein-1 (YAP) and transcriptional enhancer factor domain interaction through inhibition of the Hippo-YAP pathway to suppress the expression of targeted genes.⁴⁰ All of the above mechanisms might contribute to the efficacy of verteporfin-PDT on pancreatic cancer cells.⁸ Some studies have demonstrated that verteporfin could be delivered to cancer cells with a much shorter

time interval between drug administration and photoactivation and with less photosensitivity than the older generation photosensitizers.^{8,41,42}

Our study confirmed that sodium porfimer and verteporfin-PDT induced death in pancreatic cancer in a dose-dependent manner as reported by other groups.^{3,9,35} In this study, we observed that all cell lines had nonresponsive populations at lower and moderate doses of both the photosensitizers. We showed that HNPE exhibited significantly higher sensitivity to PDT than multiple pancreatic cancer cell lines [Figs. 2(a) and 2(b)]. While the LD50 of pancreatic cell lines for sodium porfimer and verteporfin-PDT showed a similar effect, the sensitivity of cancer cell lines to these PDTs exhibited a different grade of responsiveness, in order from high to low sensitivity as follows: HPNE, PANC-1, BxPC-3, MIA PaCa-2, and CAPAN-2. Since HPNE cells have a normal pancreatic duct epithelium phenotype,²⁸ we may conclude that normal pancreatic duct epithelial cells are fairly sensitive to PDT. This might have important implications for clinical PDT treatment, as extra measures to avoid injury to normal pancreatic tissue might be needed.

When comparing different concentrations of sodium porfimer PDT, the cell death rates between the pancreatic cancer lines were not significantly different, suggesting that sodium porfimer PDT is not selective for any particular subtype of pancreatic cancer cells. In contrast, verteporfin-PDT showed variable efficacy of cell death in those four pancreatic cancer cell lines tested. BxPC-3 (adenosquamous) was more sensitive than other cells at lower concentrations of verteporfin-PDT, while CAPAN-2 (moderately differentiated) was the least sensitive [Figs. 2(b) and 2(d)]. PANC-1 and MIA PaCa-2, the two adenocarcinoma lines with poor histologic differentiations, showed greater and lesser sensitivities, respectively, to verteporfin-PDT than BxPC-3. The cytotoxic response to PDT depends on the intracellular uptake and localization of the photosensitizers. Celli et al.¹⁰ have reported a differential uptake of verteporfin by various pancreatic cancer cell lines. BxPC-3 had a peak of maximum level of total verteporfin in $\mu\text{mol}/\text{mg}$ regime in contrast to PANC-1 and CAPAN-2 cells, which showed lower uptake peak of verteporfin in the range of 200 to 400 nmol/mg 6 h of post-PDT.¹⁰ In this study, the differential cytotoxic response of verteporfin-PDT among the various types of pancreatic cancer cells correlates with the different PDT uptake rates *in vitro*. These data altogether suggest that cellular uptake of photosensitizers has been critical for drug response and resistance to cytotoxicity. In addition, factors such as the oxygen dependence of photosensitizing effect also play an important role in PDT-mediated therapy. The singlet oxygen ($^1\text{O}_2$) produced by the reaction of photoexcited porphyrin molecules with oxygen molecules in tumor cells⁴³ involves the oxygen dependence of the photosensitizing effect of photosensitizers. Moan and Sommer⁴⁴ reported the quantum yield of sodium porfimer to be about 0.9 relative unit at oxygen concentrations of 0.07 mM. However, the study was performed on sodium porfimer at lower concentrations than those used for clinical applications, and the drug dosages given are far in excess of the levels required for maximal singlet oxygen generation. Therefore, in most clinical situations, quantum efficiency of the drug does not appear to be a limiting factor in PDT-induced cell death. Among other factors, vascular permeability also plays an important role in selective accumulation and drug penetration.⁴⁵ A study has shown that the increase in distance of cells from the vascular supply diminished the accumulation and effectiveness of intravenously administered photosensitizers.⁴⁶ The availability of oxygen within the target tissue limits direct tumor destruction by accumulated photosensitizers. Depending on the spatial availability of photosensitizers, oxygen tension can increase transiently.⁴⁷ Altogether, this study brings to light some provocative explanations of how the sensitivity of the two photosensitizers varies in terms of PDT response with different cell types, requiring further investigation in the context of photophysical, chemical, quantum efficiency, and biological properties (i.e., cellular uptake, distribution, and tumor selectivity), and more complex preclinical models are needed to establish the role of PDT on pancreatic cancer research.

It is important to understand the genetic factors that lead to resistance to chemotherapy in pancreatic cancer. It is known that KRAS, TP53, CDKN2A, and SMAD4 mutation are the classic genetic mutations found in pancreatic cancer, but also some rare genetic mutations, such as MLL3, BCLAF1, IRF6, FLG, AXIN1, GLI3, PIK3CA, RBM TGFBR2, ARID1A, EPC1, ARID2, SF3B1, ATM, and RNF43, occur, causing increased genomic heterogeneity between pancreatic cancers.⁴⁸ The stage

of pancreatic cancer is associated with different mutations, with KRAS, p16/CDKN2A, GNAS, and BRAF being mutated in early phases of pancreatic cancer, while SMAD4/DPC4 and TP53 are mutated in later stages.^{49–52} The cell lines used in this study, PANC-1, BxPC-3, MIA PaCa-2, and CAPAN-2, were derived from different pancreatic cancer patients and showed different biological and genetic characteristics. For example, MIA PaCa-2 and PANC-1, derived from undifferentiated pancreatic carcinoma, are highly aggressive cell lines with increased intrinsic ZEB1 expression, known to correlate with poor prognosis.^{53,54} Both cell lines were reported to have KRAS and TP53 mutations and P16 homozygous deletions.³⁵ CAPAN-2 also has a KRAS mutation and BxPC-3 has CDKN2A, MAP2K4, SMAD4, and TP53 mutations.¹⁸ Such genetic heterogeneity might contribute to the diverse effects of treatment with photosensitizers. Furthermore, the different cellular functions may influence the effect of PDT treatment. For example, CAPAN-2 and BxPC-3 cells are known to produce mucin, which is shown to be correlated with chemoresistance via activating multidrug resistance genes⁵⁵ and possibly is also correlated with resistance to PDT.

Using different pancreatic cell lines and with comparable illumination regimens, we performed a comparative study of the basic PDT-related characteristics between the two photosensitizers and provide important parameters on the pancreatic model. Variable sensitivity to the PDT therapy among different grades of pancreatic cancer cell lines provides basic insight into selecting more appropriate photosensitizer for clinical purposes. In light of the noted importance of the tumor microenvironment and specifically interaction with the stromal component, in this study, we used stimulated fibroblasts and HPSCs inserts and incubated with PANC-1. The increased expression level of α -SMA verified effective stimulation of the fibroblasts and HPSCs, leading to a myofibroblast-like phenotype that was maintained throughout the experiment. Our hypothesis in this study was that stimulated fibroblasts or HPSCs might have some protective effects toward PANC-1 against PDT treatment. The existing studies have shown the complex roles of fibroblasts in the tumor microenvironment. Once stimulated, fibroblasts and PSCs may interact with tumor cells through various mechanisms, leading to tumor growth, invasion and metastasis, and chemoresistance.^{27,33,54} Results showed that PANC-1 cells were sensitive to verteporfin-PDT. Furthermore, any reduction of cytotoxicity of verteporfin-PDT by stimulated fibroblasts or HPSCs in co-cultures with PANC-1 cells was not observed, which is consistent with one prior study done only in a two-dimensional culture.³¹ Verteporfin-PDT treatment on PANC-1, co-cultured with either stimulated HPSCs or stimulated fibroblasts, demonstrated a similar effect, indicating that both fibroblasts and HPSCs perform a very similar role *in vitro* and that there is no tissue-specific difference between these stromal cells. However, *in-vitro* models do not entirely mimic the tumor microenvironment, so further studies are needed *in vivo*. Finally, Fujiwara et al.⁵⁶ demonstrated that fibroblast-rich co-cultures promoted the malignant potential of the pancreatic cancer cell line BxPC-3, both *in vitro* and *in vivo*. Celli³¹ developed 3-D co-cultures of PANC-1 with MRC-5 normal human fibroblasts derived from lung, showing that verteporfin-PDT was able to destroy fibroblasts as well as pancreatic cancer cells. The same group also demonstrated that the ECM infiltrating populations showed enhanced sensitivity

to verteporfin-PDT, despite resistance to chemotherapy.⁵⁷ The role of pancreatic stellate cells in PDT has not been extensively studied.

Surgical resection as a treatment option for pancreatic cancer has many limitations since the number of patients undergoing resection with a curative intent may drop to as low as 3%^{58,59} with the median survival being only 10 to 20 months and no more than 5% to 20% of the resected patients survive more than five years.⁶⁰ Chemotherapy, radiotherapy, and the combination of the two are the options available for the treatment of inoperable patients. Among the chemotherapeutic agents, gemcitabine is the most commonly used agent in both the US and Europe. According to the UK-based phase III randomized clinical study, the median survival in the combination capecitabine + gemcitabine has shown an improved survival rate of 7.1 months compared with those receiving gemcitabine alone (6.2 months).⁶¹ The French randomized study of FOLFIRINOX (fluorouracil, oxaliplatin, leucovorin, and irinotecan) versus gemcitabine showed a significantly improved survival rate (median 11.1 versus 6.8 months).⁶² However, the invariably poor response to chemotherapy becomes an increasing challenge due to the resistance of the pancreatic tumor cells to the mitochondria-mediated apoptotic signal^{63–65} besides many other signalling pathways.⁶⁶ Moreover, extensive fibrous stroma and the complex interactions between the components of ECM and stroma possess a physical barrier in drug delivery.^{67,68} In this study, we compare the two most proficient photosensitizers that preferentially accumulate around mitochondria to enhance efficacy and drug penetration. PDT, being a targeted anticancer therapeutic modality, has been extensively investigated for the management of dysplasia and malignancy of ampulla and pancreas and has been reported as safe, feasible, and possibly a cure for small tumors.^{15,69} Studies by Bown et al.¹⁶ suggested that the CT guided mTHPC-PDT induced tumor necrosis to 100% of the patients with pancreatic cancer without treatment-related morbidity. Very recently, sodium porfimer has been used as EUS-PDT with a combination of Nab-paclitaxel and gemcitabine in a phase I clinical trial safely and effectively on 12 locally advanced pancreatic cancer patients. In this study, 50% of the patients had responded with mean overall increase in volume and percentage of necrosis with median progression free and overall survival of 2.6 and 11.5 months.⁷⁰ However, what limits pancreatic cancer therapy with these two photosensitizers is a longer post-PDT duration of photosensitivity. Verteporfin, the second generation PDT, has been used in a phase I/II clinical trial with effective PDT-induced tumor necrosis, a much shorter drug light interval, and less photosensitivity, providing an impetus to a more convenient treatment regimen than the other compounds.^{8,71} Our study has shown that verteporfin was more effective at lower concentrations than sodium porfimer to kill the cancer cells effectively and could be a better option to select for combination therapy with gemcitabine or any other standard chemopreventive compound currently being used. Verteporfin has distinct advantages to sodium porfimer including light absorption at a longer wavelength allowing for greater tissue penetration than sodium porfimer. Moreover, because verteporfin-PDT is more effective than sodium porfimer on pancreatic cancer cells at lower and moderate doses, a wide range of sensitivity for clinical use is suggested. The stimulated fibroblasts or HPSCs, showing an enhanced myofibroblastic phenotype compared with unstimulated cells, did not show a significant protective effect on PANC-1 cells against verteporfin-PDT.

Considering the tumor diversity, it is imperative to understand which photosensitizers are more appropriate for overcoming the pancreatic tumor heterogeneity and how chemotherapeutic agents exert their efficacy when expolited together in combination therapy with PDT. Overall, our study has shown that verteporfin is relatively agnostic to pancreatic tumor type and can kill all types of pancreatic tumor based on their histology and heterogeneity. We think that the next step is to test this compound in combination with chemotherapy to determine how it can enhance the effect *in vivo*. Verteporfin with its strong absorption maxima, longer wavelength, and deep tissue penetrating capability becomes the more potential candidate for pancreatic cancer treatment. A study by Celli et al.¹⁰ demonstrated that the verteporfin in combination with gemcitabine bypassed the gemcitabine resistance in pancreatic cancer cell lines. Verteporfin-mediated regulation of YAP is critical in tumor pathophysiology where p53 is the wild type.⁷² YAP pathway is known as a major clinical determinant of tumor progression and poor survival in pancreatic cancer.⁷³ Taken together, combination therapy of verteporfin-PDT and gemcitabine as the chemopreventive agent should be tested and therefore further *in vivo* studies and preclinical testing to identify the most suitable drug combinations are required.

In conclusion, this study elucidates the potential role of PDT in the therapeutic armamentarium for pancreatic cancer, demonstrating an effective chemotherapeutic role *in vitro*, based on which a further investigation into PDT and chemotherapy in combination is warranted to overcome chemoresistance of pancreatic cancer in preclinical 3-D and *in vivo* cancer model.

Disclosures

The authors of this paper have no competing interests to declare.

Acknowledgments

HPSCs were donated by Dr. Rosa F. Hwang, the University of Texas MD Anderson Cancer Center, Houston, Texas. This work was funded by the National Institutes of Health Grant No. P01CA084203.

References

1. R. L. Siegel, K. D. Miller, and A. Jemal, "Cancer statistics, 2017," *CA Cancer J. Clin.* **67**(1), 7–30 (2017).
2. M. A. Tempero et al., "Pancreatic adenocarcinoma, Version 2.2017, NCCN clinical practice guidelines in oncology," *J. Natl. Compr. Cancer Network* **15**(8), 1028–1061 (2017).
3. G. Sun et al., "Synergistic effects of photodynamic therapy with HPPH and gemcitabine in pancreatic cancer cell lines," *Lasers Surg. Med.* **44**(9), 755–761 (2012).
4. R. R. Allison et al., "Photosensitizers in clinical PDT," *Photodiagn. Photodyn. Ther.* **1**(1), 27–42 (2004).
5. D. E. Dolmans, D. Fukumura, and R. K. Jain, "Photodynamic therapy for cancer," *Nat. Rev. Cancer* **3**(5), 380–387 (2003).
6. B. G. Fan and A. Andren-Sandberg, "Photodynamic therapy for pancreatic cancer," *Pancreas* **34**(4), 385–389 (2007).
7. J. B. Wang and L. X. Liu, "Use of photodynamic therapy in malignant lesions of stomach, bile duct, pancreas, colon and rectum," *Hepato-Gastroenterology* **54**(75), 718–724 (2007).
8. M. T. Huggett et al., "Phase I/II study of verteporfin photodynamic therapy in locally advanced pancreatic cancer," *Br. J. Cancer* **110**(7), 1698–1704 (2014).
9. Q. Xie et al., "Synergetic anticancer effect of combined gemcitabine and photodynamic therapy on pancreatic cancer *in vivo*," *World J. Gastroenterol.* **15**(6), 737–741 (2009).

10. J. P. Celli et al., "Verteporfin-based photodynamic therapy overcomes gemcitabine insensitivity in a panel of pancreatic cancer cell lines," *Lasers Surg. Med.* **43**(7), 565–574 (2011).
11. L. Ayaru, S. G. Bown, and S. P. Pereira, "Photodynamic therapy for pancreatic carcinoma: experimental and clinical studies," *Photodiagn. Photodyn. Ther.* **1**(2), 145–155 (2004).
12. H. C. Huang et al., "Photodynamic priming mitigates chemotherapeutic selection pressures and improves drug delivery," *Cancer Res.* **78**(2), 558–571 (2018).
13. G. Shafirstein et al., "Interstitial photodynamic therapy—a focused review," *Cancers* **9**(2), 12 (2017).
14. K. T. Moesta et al., "Evaluating the role of photodynamic therapy in the management of pancreatic cancer," *Lasers Surg. Med.* **16**(1), 84–92 (1995).
15. H. H. Chan et al., "EUS-guided photodynamic therapy of the pancreas: a pilot study," *Gastrointest. Endosc.* **59**(1), 95–99 (2004).
16. S. G. Bown et al., "Photodynamic therapy for cancer of the pancreas," *Gut* **50**(4), 549–557 (2002).
17. M. Topazian et al., "Photodynamic therapy of intraductal papillary mucinous neoplasm," *Endoscopy* **44**(2), 213–215 (2012).
18. E. L. Deer et al., "Phenotype and genotype of pancreatic cancer cell lines," *Pancreas* **39**(4), 425–435 (2010).
19. B. Sipos et al., "A comprehensive characterization of pancreatic ductal carcinoma cell lines: towards the establishment of an in vitro research platform," *Virchows Arch.* **442**(5), 444–452 (2003).
20. P. Loukopoulos et al., "Orthotopic transplantation models of pancreatic adenocarcinoma derived from cell lines and primary tumors and displaying varying metastatic activity," *Pancreas* **29**(3), 193–203 (2004).
21. G. Berzoppe et al., "Comparative analysis of mutations in the p53 and K-ras genes in pancreatic cancer," *Int. J. Cancer* **58**(2), 185–191 (1994).
22. P. S. Moore et al., "Genetic profile of 22 pancreatic carcinoma cell lines. Analysis of K-ras, p53, p16 and DPC4/Smad4," *Virchows Arch.* **439**(6), 798–802 (2001).
23. C. Sun et al., "Characterization of the mutations of the K-ras, p53, p16, and SMAD4 genes in 15 human pancreatic cancer cell lines," *Oncol. Rep.* **8**(1), 89–181 (2001).
24. J. Butz, E. Wickstrom, and J. Edwards, "Characterization of mutations and loss of heterozygosity of p53 and K-ras2 in pancreatic cancer cell lines by immobilized polymerase chain reaction," *BMC Biotechnol.* **3**, 11 (2003).
25. S. Kaur et al., "Mucins in pancreatic cancer and its microenvironment," *Nat. Rev. Gastroenterol. Hepatol.* **10**(10), 607–620 (2013).
26. N. Remmers et al., "Aberrant expression of mucin core proteins and O-linked glycans associated with progression of pancreatic cancer," *Clin. Cancer Res.* **19**(8), 1981–1993 (2013).
27. D. von Ahrens et al., "The role of stromal cancer-associated fibroblasts in pancreatic cancer," *J. Hematol. Oncol.* **10**(1), 76 (2017).
28. S. Suklabaidya, P. Dash, and S. Senapati, "Pancreatic fibroblast exosomes regulate survival of cancer cells," *Oncogene* **36**(25), 3648–3649 (2017).
29. L. G. Melstrom, M. D. Salazar, and D. J. Diamond, "The pancreatic cancer microenvironment: a true double agent," *J. Surg. Oncol.* **116**(1), 7–15 (2017).
30. M. Waghray et al., "Deciphering the role of stroma in pancreatic cancer," *Curr. Opin. Gastroenterol.* **29**(5), 537–543 (2013).
31. J. P. Celli, "Stromal interactions as regulators of tumor growth and therapeutic response: a potential target for photodynamic therapy?" *Isr. J. Chem.* **52**(8–9), 757–766 (2012).
32. M. C. Palanca-Wessels et al., "Genetic analysis of long-term Barrett's esophagus epithelial cultures exhibiting cytogenetic and ploidy abnormalities," *Gastroenterology* **114**(2), 295–304 (1998).
33. R. F. Hwang et al., "Cancer-associated stromal fibroblasts promote pancreatic tumor progression," *Cancer Res.* **68**(3), 918–926 (2008).
34. G. Buniatian, B. Hamprecht, and R. Gebhardt, "Glial fibrillary acidic protein as a marker of perisinusoidal stellate cells that can distinguish between the normal and myofibroblast-like phenotypes," *Biol. Cell* **87**(1–2), 65–73 (1996).
35. L. W. Wang et al., "Effect of Photofrin-mediated photocytotoxicity on a panel of human pancreatic cancer cells," *Photodiagn. Photodyn. Ther.* **10**(3), 244–251 (2013).
36. V. G. Schweitzer, "Photofrin-mediated photodynamic therapy for treatment of early stage oral cavity and laryngeal malignancies," *Lasers Surg. Med.* **29**(4), 305–313 (2001).
37. M. Stoodley and J. M. Sikorski, "Objective and useful mobility assessment of patients with arthropathy of the hip and knee," *Clin. Orthop. Relat. Res.* **224**, 110–116 (1987).
38. I. Banti et al., "Synthesis and in-vitro antitumor activity of new naphthridine derivatives on human pancreatic cancer cells," *J. Pharm. Pharmacol.* **61**(8), 1057–1066 (2009).
39. L. Ayaru et al., "Photodynamic therapy using verteporfin photosensitization in the pancreas and surrounding tissues in the Syrian golden hamster," *Pancreatol.* **7**(1), 20–27 (2007).
40. H. Wei et al., "Verteporfin suppresses cell survival, angiogenesis and vasculogenic mimicry of pancreatic ductal adenocarcinoma via disrupting the YAP-TEAD complex," *Cancer Sci.* **108**(3), 478–487 (2017).
41. V. E. Gomez, E. Giovannetti, and G. J. Peters, "Unraveling the complexity of autophagy: potential therapeutic applications in pancreatic ductal adenocarcinoma," *Semin Cancer Biol.* **35**, 11–19 (2015).
42. E. Donohue et al., "The autophagy inhibitor verteporfin moderately enhances the antitumor activity of gemcitabine in a pancreatic ductal adenocarcinoma model," *J. Cancer* **4**(7), 585–596 (2013).
43. K. R. Weishaupt, C. J. Gomer, and T. J. Dougherty, "Identification of singlet oxygen as the cytotoxic agent in photo-inactivation of a murine tumor," *Cancer Res.* **36**(7 Pt. 1), 2326–2329 (1976).
44. J. Moan and S. Sommer, "Oxygen dependence of the photosensitizing effect of hematoporphyrin derivative in NHIK 3025 cells," *Cancer Res.* **45**(4), 1608–1610 (1985).
45. T. J. Dougherty et al., "Photodynamic therapy," *J. Natl. Cancer Inst.* **90**(12), 889–905 (1998).
46. M. Korbelik and G. Krosli, "Cellular levels of photosensitizers in tumours: the role of proximity to the blood supply," *Br. J. Cancer* **70**(4), 604–610 (1994).
47. B. W. Pogue et al., "Photodynamic therapy with verteporfin in the radiation-induced fibrosarcoma-1 tumor causes enhanced radiation sensitivity," *Cancer Res.* **63**(5), 1025–1033 (2003).
48. F. Notta, S. A. Hahn, and F. X. Real, "A genetic roadmap of pancreatic cancer: still evolving," *Gut* **66**(12), 2170–2178 (2017).
49. F. Ruckert et al., "Five primary human pancreatic adenocarcinoma cell lines established by the outgrowth method," *J. Surg. Res.* **172**(1), 29–39 (2012).
50. M. Kanda et al., "Presence of somatic mutations in most early-stage pancreatic intraepithelial neoplasia," *Gastroenterology* **142**(4), 730–733.e9 (2012).
51. H. Hayashi et al., "Utility of assessing the number of mutated KRAS, CDKN2A, TP53, and SMAD4 genes using a targeted deep sequencing assay as a prognostic biomarker for pancreatic cancer," *Pancreas* **46**(3), 335–340 (2017).
52. S. H. Shin et al., "The DPC4/SMAD4 genetic status determines recurrence patterns and treatment outcomes in resected pancreatic ductal adenocarcinoma: a prospective cohort study," *Oncotarget* **8**(11), 17945–17959 (2017).
53. U. Wellner et al., "The EMT-activator ZEB1 promotes tumorigenicity by repressing stemness-inhibiting microRNAs," *Nat. Cell Biol.* **11**(12), 1487–1495 (2009).
54. L. Bolm et al., "The role of fibroblasts in pancreatic cancer: extracellular matrix versus paracrine factors," *Transl. Oncol.* **10**(4), 578–588 (2017).
55. S. Nath et al., "MUC1 induces drug resistance in pancreatic cancer cells via upregulation of multidrug resistance genes," *Oncogenesis* **2**, e51 (2013).
56. M. Fujiwara et al., "ASF-4-1 fibroblast-rich culture increases chemoresistance and mTOR expression of pancreatic cancer BxPC-3 cells at the invasive front in vitro, and promotes tumor growth and invasion in vivo," *Oncol. Lett.* **11**(4), 2773–2779 (2016).
57. G. M. Cramer et al., "ECM composition and rheology regulate growth, motility, and response to photodynamic therapy in 3D models of pancreatic ductal adenocarcinoma," *Mol. Cancer Res.* **15**(1), 15–25 (2017).
58. S. M. de Castro et al., "Incidence and characteristics of chronic and lymphoplasmacytic sclerosing pancreatitis in patients scheduled to undergo a pancreatoduodenectomy," *HPB* **12**(1), 15–21 (2010).
59. A. L. Warshaw and C. Fernandez-del Castillo, "Pancreatic carcinoma," *N. Engl. J. Med.* **326**(7), 455–465 (1992).
60. A. Stojadinovic et al., "An evidence-based approach to the surgical management of resectable pancreatic adenocarcinoma," *J. Am. Coll. Surg.* **196**(6), 954–964 (2003).

61. D. Cunningham et al., "Phase III randomized comparison of gemcitabine versus gemcitabine plus capecitabine in patients with advanced pancreatic cancer," *J. Clin. Oncol.* **27**(33), 5513–5518 (2009).
62. T. Conroy et al., "FOLFIRINOX versus gemcitabine for metastatic pancreatic cancer," *N. Engl. J. Med.* **364**(19), 1817–1825 (2011).
63. I. Petak and J. A. Houghton, "Shared pathways: death receptors and cytotoxic drugs in cancer therapy," *Pathol. Oncol. Res.* **7**(2), 95–106 (2001).
64. B. Schniewind et al., "Resistance of pancreatic cancer to gemcitabine treatment is dependent on mitochondria-mediated apoptosis," *Int. J. Cancer* **109**(2), 182–188 (2004).
65. R. J. Bold, J. Chandra, and D. J. McConkey, "Gemcitabine-induced programmed cell death (apoptosis) of human pancreatic carcinoma is determined by Bcl-2 content," *Ann. Surg. Oncol.* **6**(3), 279–285 (1999).
66. K. Koizumi et al., "Activation of p38 mitogen-activated protein kinase is necessary for gemcitabine-induced cytotoxicity in human pancreatic cancer cells," *Anticancer Res.* **25**(5), 3347–3353 (2005).
67. A. Neesse et al., "Stromal biology and therapy in pancreatic cancer: a changing paradigm," *Gut* **64**(9), 1476–1484 (2015).
68. A. Neesse et al., "Stromal biology and therapy in pancreatic cancer: ready for clinical translation?" *Gut* **68**(1), 159–171 (2019).
69. C. D. Liu et al., "Hypericin and photodynamic therapy decreases human pancreatic cancer *in vitro* and *in vivo*," *J. Surg. Res.* **93**(1), 137–143 (2000).
70. J. M. DeWitt et al., "Phase I study of EUS-guided photodynamic therapy for locally advanced pancreatic cancer," *Gastrointest. Endosc.* **89**(2), 390–398 (2019).
71. M. Jermyn et al., "CT contrast predicts pancreatic cancer treatment response to verteporfin-based photodynamic therapy," *Phys. Med. Biol.* **59**(8), 1911–1921 (2014).
72. C. Wang et al., "Verteporfin inhibits YAP function through up-regulating 14-3-3 σ sequestering YAP in the cytoplasm," *Am. J. Cancer Res.* **6**(1), 27–37 (2016).
73. E. Rozengurt, J. Sinnott-Smith, and G. Eibl, "Yes-associated protein (YAP) in pancreatic cancer: at the epicenter of a targetable signaling network associated with patient survival," *Signal Transduction Targeted Ther.* **3**, 11 (2018).

Kenneth K. Wang is the Russ and Kathy Van Cleve Professor of Gastroenterology Research at the Mayo Clinic Rochester, Minnesota, where he conducts translational research programs in gastrointestinal neoplasms including pancreatic and esophageal cancer. He has been involved in phototherapy for the past 20 years.

Biographies of the other authors are not available.